DFT and ab Initio Study of the Unimolecular Decomposition of the Lowest Singlet and Triplet States of Nitromethane

M. Riad Manaa* and Laurence E. Fried†

Lawrence Livermore National Laboratory, Chemistry and Materials Science Directorate, P.O. Box 808, L-282, Livermore, California 94551

Received: April 27, 1998; In Final Form: August 24, 1998

The fully optimized potential energy curves for the unimolecular decomposition of the lowest singlet and triplet states of nitromethane through the C−NO_2 bond dissociation pathway are calculated using various DFT and high-level ab initio electronic structure methods. We perform gradient corrected density functional theory (DFT) and multiconfiguration self-consistent field (MCSCF) to conclusively demonstrate that the triplet state of nitromethane is bound. The adiabatic curve of this state exhibits a 33 kcal/mol energy barrier as determined at the MCSCF level. DFT methods locate this barrier at a shorter C−N bond distance with 12−16 kcal/mol lower energy than does MCSCF. In addition to MCSCF and DFT, quadratic configuration interactions with single and double substitutions (QCISD) calculations are also performed for the singlet curve. The potential energy profiles of this state predicted by DFT methods based on Becke's 1988 exchange functional differ by as much as 17 kcal/mol from the predictions of MCSCF and QCISD in the vicinity of the equilibrium structure. The computational methods predict bond dissociation energies 5−9 kcal/mol lower than the experimental value. DFT techniques based on Becke's 3-parameter exchange functional show the best overall agreement with the higher level methods.

Introduction

Nitromethane is the simplest nitro compound. As a prototypical energetic molecule of modest size, its energetic and structural properties are amenable to detailed and high-level computational treatments. Such properties could then be benchmarked to other efficient methods capable of handling large energetic systems, which typically consist of 20−50 atoms.[1,2] Furthermore, knowledge of the excited potential energy surfaces of nitromethane would prove useful in elucidating some of its photochemistry. In the present paper, we undertake a systematic study of the C−N bond dissociation in nitromethane via the singlet and triplet electronic states, comparing density functional theory (DFT) to multiconfiguration self-consistent field (MCSCF) and quadratic configuration interaction (QCI) methods.

DFT methods are efficient techniques capable of treating electron correlation in moderately large systems. Numerous studies comparing these methods now exist in the literature (for example, see refs 3−5). Recent studies have shown that approximate functionals take into account most of the dynamical and static electron correlation effects, thus producing descriptions of molecular spectroscopic properties of comparable quality to more expensive correlated methods.[6−9] Relatively few comparative studies, however, have been performed to locate transition states and predict reaction paths.[10] Such investigations are highly desirable in order to establish the limitations of DFT methods across wide regions of the molecular potential energy surface before subsequent dynamics simulations are performed. Moreover, it is important to document the performance of DFT methods in describing a closed-shell system (singlet) and an open-shell counterpart (triplet) on an equal footing. To date very few DFT calculations for both states have been performed.[11−13] Only a few previous studies have compared the MCSCF method to DFT.[14,15] To our knowledge, the present work is the first study to compare DFT calculations to MCSCF results in a full optimization of a homolytic bond dissociation curve for both the singlet and triplet states of a polyatomic molecule.

Many experimental and theoretical studies under both normal and extreme thermodynamic conditions have been performed on nitromethane. Recent experimental studies on liquid nitromethane have suggested bimolecular[16,17] or ionic[18] decomposition mechanisms to be operative under shock conditions. Studies concerning the vibrational spectra of the liquid phase are numerous and sometimes conflicting.[19−22] On the other hand, photodissociation studies have shown that cleavage of the C−N bond to yield the methyl radical and nitrogen dioxide is the primary decomposition process in the gas phase.[23] The lowest singlet → triplet excitation in nitromethane was reported by electron-impact spectroscopy[24] with the observed transition having an onset at 3.1 eV and a maximum intensity at 3.8 eV. The authors have concluded that the transition plays an important role in the gas-phase photolysis of nitromethane, supporting an earlier claim that photolysis leading to CH_3 and NO_2 occurs via a triplet intermediate.[25] The role of a nonradiative deexcitation channel from the excited to the ground state has also been observed,[26] suggesting the need for a further characterization of the excited states of this molecule.

Computationally, a recent DFT study reported[27] a few geometric parameters for the equilibrium structure of the triplet state. The potential energy surfaces of the low-lying singlet and triplet states of nitromethane for the C−N decomposition pathway were determined by Rosak and Kaufman using multireference double excitation configuration interaction.[28] They constrained the molecule to C_s symmetry, and held both the C−H and N−O bonds fixed throughout the optimization

† E-mail: manaa1@llnl.gov, lfried@llnl.gov.

10.1021/jp982003s CCC: $15.00
Published on Web 11/26/1998

procedure. A fully optimized calculation is very important in understanding the dissociation via the triplet surface, since this state has an equilibrium geometric structure markedly different from that of the ground state. Molecular dynamics simulations of liquid nitromethane under ambient and shocked conditions were performed by Seminario et al.[29] using a force field determined from DFT calculations. A very recent study reported ab initio (DFT) molecular dynamics of solid nitromethane.[30] Many other theoretical studies concentrated on alternative decomposition pathways on the ground-state surface.[31−33]

In this work, various DFT methods are compared to MCSCF calculations for the singlet and triplet states of nitromethane through C−NO_2 dissociation pathway. We use the complete active space self-consistent field (CASSCF)[34] variant of MCSCF, a method that is capable of treating homolytic bond dissociation without spin contamination of the wave function. Nevertheless, this method is not size consistent. We have thus chosen the QCI method with single and double substitution (QCISD)[35] which offers results of quality comparable to coupled cluster theory. Our calculations are based on a fully optimized reaction. The profile of the potential energy curve could be used in interpreting vibrational spectroscopy performed on nitromethane through the C−N stretching mode.[19−22,29] We also show here that the triplet state is bound, with a barrier of roughly 33 kcal/mol. These results suggest that the triplet state should support several vibrational states, unless radiationless decay mechanisms (currently under study)[36] are operative at low vibrational excitations. Finally, the comparative calculations allow us to reach definitive conclusions regarding the applicability of DFT methods to homolytic bond dissociation in energetic materials.

Computational Methods

DFT and MCSCF calculations were performed on both singlet and triplet states. For the singlet state, QCISD calculations are also included. In all calculations the C−N bond distance was fixed at a certain value while the rest of the molecular parameters were optimized. The tilting angle ϕ is defined as the deviation of the ONO plane from the vertical line that passes through the C−N bond. The potential energy surface was calculated in the range of R(CN) = 1.5−4.0 Å at a 0.25 Å interval with two additional points at 1.3 and 1.4 Å were also performed for the ground-state singlet. Additional points were calculated for the triplet state near the "transition" state. The equilibrium structure of nitromethane, NO_2, and CH_3 were determined along with the harmonic frequencies to include the zero point correction to the dissociation energy. The DFT and QCISD calculations have been performed using the GAUSSIAN94 package of codes[37] with its default convergence criteria for the energies and wave functions. The DFT and QCISD based wave functions were spin unrestricted to ensure proper behavior at large bond distances. The onset of spin contamination in the unrestricted calculations was monitored.

We chose four different functionals for the DFT calculations of the singlet state. The hybrid B3PW91 and B3LYP methods refer to Becke's three-parameter exchange functional[38] along with the nonlocal correlation of Perdew−Wang[39] and Lee−Yang−Parr[40] functionals, respectively. The nonlocal methods BPW91 and BLYP are a combination of Becke's 1988 exchange functional[41] and the correlation functionals mentioned above. For the triplet state, the B3LYP and BLYP functionals were employed.

We used the GAMESS[42] program for the MCSCF calculations. The active space was based on six electrons distributed in five orbitals. At the equilibrium geometry the molecule has C_s symmetry with a dominant single closed-shell configuration character and mixed with a second configuration.[28,43] The active space represents three occupied orbitals: the CN (σ), the "in-plane" NO_2, and the NO_2 (π) orbitals. As the CN bond stretches, the wave function becomes strongly multideterminental, with the singlet potential surface approaching the dissociating triplet surface. In this region, the electrons are distributed between both the occupied space (described above) and two unoccupied orbitals, the CN (σ^*) and NO_2 (π^*) molecular orbitals. The chosen active space allows for a proper description of molecular dissociation into two open-shell fragments, CH_3 and NO_2, with which both the singlet and triplet states correlate.

The molecular orbitals were expanded in terms of two standard atomic basis sets. The 6-311G** (C, N, O, 4s3p1d; H, 3s1p) basis was employed for the singlet surface with all the computational procedures of this work. The larger 6-311++G(2d,2p) (C, N, O, 5s4p2d; H, 4s2p) basis was implemented at selected geometries and in conjunction with the DFT and the MCSCF methods for both the singlet and triplet surfaces.

TABLE 1: Triplet and Singlet (Bottom Values) State Equilibrium Structures and Total Energies (E_e, in Hartrees) Determined with the 6-311++G(2d,2p) Basis Set with Bond Lengths in Å and Angles in deg

	MCSCF	B3LYP	BLYP
R(C−H_1)	1.082	1.091	1.098
	1.080	1.087	1.094
R(C−$H_{2,3}$)	1.077	1.086	1.094
	1.075	1.083	1.090
R(C−N)	1.487	1.464	1.476
	1.508	1.498	1.519
R(N−O)	1.302	1.309	1.330
	1.197	1.221	1.241
∠H_2CH_1	110.3	110.7	110.8
	110.9	110.2	110.3
∠NCH_1	110.7	109.4	109.6
	106.9	106.6	106.5
∠$NCH_{2,3}$	107.5	107.8	107.6
	107.6	108.0	107.9
∠CNO	114.2	118.4	118.8
	117.3	117.3	117.1
∠ONO	111.7	105.3	104.9
	125.5	125.7	125.7
∠ϕ	48.6	44.8	44.4
	1.6	1.4	1.4
E_e	−243.714 626	−245.009 367	−244.976 374
	−243.815 391	−245.102 417	−245.067 107
ZPE	31.6	29.5	28.6
	33.4	31.2	30.0

Results and Discussion

The Triplet State. As noted in the Introduction, the only experimental study of the spin-forbidden singlet → triplet excitation was reported by electron-impact spectroscopy[24] with the observed transition having an onset at 3.1 eV and a maximum intensity at 3.8 eV. This state correlates asymptotically with the ground-state singlet, yielding the CH_3 and NO_2 radicals. Despite the claim that the electronic transition plays an important role in the gas-phase photolysis of nitromethane,[24,25] spectroscopic parameters have not been identified for the triplet state. A recent DFT comparative study[27] provided only three structural parameters: R(C−N), R(N−O), and the ∠CNO. Table 1 provides the geometric parameters of the minimum for both the triplet and singlet states at the MCSCF, B3LYP, and BLYP levels. For the triplet state, the NO_2 group arrangement

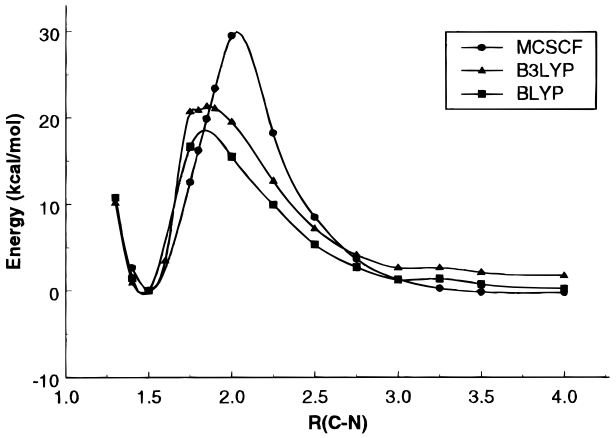

Figure 1. Fully optimized DFT and MCSCF potential energy curves of the triplet state.

TABLE 2: MCSCF and DFT(B3LYP) Harmonic Frequencies (in cm^{-1}) for the Triplet State of CH_3NO_2 with the 6-311++G(2d,2p) Basis with IR Intensities (in km/mol) in Parentheses

description	MCSCF	B3LYP	description	MCSCF	B3LYP
CN torsion	188	188 (0)	NO_2 stretch	1356	1335 (19)
NO_2 rock	446	406 (2)	CH_3 umbrella	1541	1430 (0)
NO_2 wag	463	435 (15)	HCH bend	1601	1477 (13)
NO_2 scissor	620	521 (14)	CH_3 rock	1613	1479 (17)
CN stretch	904	849 (1)	CH_3 stretch	3207	3050 (7)
NO_2 stretch	1045	872 (6)	CH_3 stretch	3285	3137 (5)
CH_3 rock	1219	1127 (9)	CH_3 stretch	3321	3163 (0)
CH_3 twist	1274	1161 (12)			

is strikingly different from the singlet equilibrium structure. The N−O bond distance is stretched by about 0.1 Å, and the ONO angle is decreased by about 10°. The two N−O bonds are no longer in the plane, with the ϕ being approximately 50°. The MCSCF wave function shows a dominant configuration with a $\pi \rightarrow \pi^*$ excitation of the NO_2 molecular orbitals. The B3LYP and BLYP calculated parameters are very close to one another, and are in close agreement with the MCSCF values. The only noticeable deviation is a decrease of ∼6° in the ONO angle and 0.02 Å in the C−N bond as determined by the DFT (B3LYP) method. The singlet−triplet (0−0) energy difference is 2.66 eV (MCSCF), 2.46 eV (B3LYP), and 2.41 eV (BLYP), all comparing well with recent results.[27] It should be noted that this energy difference is on the order of the dissociation energy of the ground state (2.6 eV), suggesting a possible role for this state in the decomposition mechanism of nitromethane.

Table 2 lists the harmonic frequencies of the triplet state minimum structure with an approximate description of each vibrational mode. All modes are positive, as expected for a true minimum, with the lowest mode attributed to the C−N torsion. The B3LYP and MCSCF values are within acceptable deviation, the maximum being ∼150 cm^{-1} in the higher modes, reflecting the difference in the calculated geometric parameters. Comparison can be made with the three vibrational frequencies provided by Jursic,[27] which at the B3LYP/6-31G(d) level are listed as 1351, 1504, and 3070 cm^{-1}. These compare well with our B3LYP-determined NO_2 stretch, CH_3 rock, and CH_3 stretch. Infrared intensities show that three strong absorption peaks are associated with the NO_2 group.

Figure 1 illustrates the fully optimized potential energy curves for the triplet state, determined from MCSCF and DFT methods. As shown, this state is bound with respect to C−N dissociation by an energy barrier of roughly 33 kcal/mol (MCSCF), 21 kcal/mol (B3LYP), and 17 kcal/mol (BLYP). The magnitude of this barrier is on the order of the zero point energy of the triplet state as determined at the MCSCF level. The energy discrepancy between the MCSCF and DFT values is ∼10 kcal/mol and, as it will be shown, of the same order as for the singlet state in the C−N bond distance range 2.0−2.25 Å. Furthermore, the location of this barrier is shifted toward larger C−N bond distance at the MCSCF level (2.0 Å) than it is at the DFT levels (1.75 Å). Table 3 lists the geometrical parameters from both MSCSF and DFT(B3LYP) calculations. We have chosen the region up to R(C−N) = 2.75 Å as a cutoff since at this point the dissociation process seems to be almost complete and beyond which the molecular parameters no longer vary in an appreciable way. As can be seen, the B3LYP parameters are in close agreement with the MCSCF results except for the noted difference in R(N−O) and ∠ONO. Finally, we note that the existence of the energy barrier renders the triplet state adiabatically stable with respect to the C−N bond dissociation, supporting a few vibrational energy levels. We are currently considering the interaction of this state near its equilibrium structure with the lower singlet. A full account of this nonadiabatic channel and its effects on the initiation process in energetic materials in general will be provided soon elsewhere.[36]

TABLE 3: Geometries and Energy Differences for the Triplet State Predicted by the DFT(B3LYP) (Top Value) and MCSCF (Bottom Value) Methods with the 6-311++G(2d,2p) Basis Set[a]

	R(C−N)						
	1.40	1.50	1.75	2.00	2.25	2.50	2.75
$R(C-H_1)$	1.094	1.089	1.082	1.079	1.078	1.078	1.078
	1.085	1.081	1.076	1.074	1.071	1.071	1.070
$R(C-H_{2,3})$	1.088	1.086	1.080	1.079	1.078	1.078	1.078
	1.078	1.077	1.074	1.073	1.071	1.070	1.070
R(N−O)	1.310	1.308	1.271	1.232	1.208	1.199	1.196
	1.303	1.301	1.298	1.287	1.170	1.167	1.166
$\angle H_2CH_1$	109.7	111.2	115.1	117.6	119.0	119.6	119.9
	109.0	110.5	113.4	115.5	118.3	119.1	119.1
$\angle NCH_1$	110.7	108.7	103.3	98.7	95.1	92.7	85.3
	112.2	110.5	106.5	103.5	97.8	93.4	86.9
$\angle CNO_1$	119.6	117.9	104.5	102.1	101.2	100.5	100.4
	115.4	114.0	111.0	108.2	100.8	100.6	100.7
∠ONO	105.2	105.3	129.2	130.9	132.4	133.4	133.9
	111.7	111.7	111.3	110.4	133.9	134.5	134.8
$\angle\phi$	42.1	46.1	56.9	62.0	63.4	64.3	64.1
	45.6	49.0	55.8	61.7	63.0	64.7	67.1
ΔE_e	1.0	0.0	20.7	19.5	12.7	7.2	4.2
	2.7	0.0	12.5	29.5	18.2	8.5	3.6

[a] Bond lengths in Å and angles in degrees. Energies are in kcal/mol relative to the near respective equilibrium structures at R(C−N) = 1.5 Å.

The Singlet State. The equilibrium structure of the ground state of nitromethane has been determined previously at various computational levels.[27,44] For this state comparisons are possible to both experiments and theory. We carried out the optimizations with the two basis sets. Optimizations were carried out only with the 6-311G** basis set for the QCISD method. In all cases the optimized geometry of nitromethane has C_s symmetry, as found previously.[27,44−47] As listed in Table 1, the tilting angle ϕ is found to be near zero. The results are in very good agreement when compared with the very recent theoretical work of Gutsev and Bartlett[44] and with the (limited) available experimental data.[47] The only noticeable deviation is the shortened MCSCF C−H and N−O bond lengths by about 0.01and 0.03 Å, respectively. The MCSCF wave function at the equilibrium structure exhibits a dominant closed-shell character, along with some mixing of configurations arising from the ($\pi-\pi^*$) excitation. The use of the larger 6-311++G(2d,2p)

TABLE 4: Dissociation Energy (Zero-Point Correction Included) in kcal/mol for the Singlet State with Results of the 6-311++G(2d,2p) Basis Below Those of the 6-311G Basis**

	B3PW91	B3LYP	BPW91	BLYP	QCISD	MCSCF	experiment
D_0	53.8	52.5	51.8	49.9	51.1	53.6	59.4
	54.5	53.4	52.4	52.9		54.4	60.1[b]
						56.2[c]	

[a] From ref 49. [b] From ref 50. [c] Calculated at R(C−N) = 8.00 Å with the 6-311++G(2d,2p) basis using the experimental data R(N−O) = 1.194 Å, ∠ONO = 133.8° for NO_2 (ref 53), and R(C−H) = 1.079 Å for CH_3 (ref 54).

basis does not have an appreciable effect on the molecular geometry with any of the methods employed. For further comparison, the calculated dipole moment is 3.67 D as determined from both MCSCF and B3LYP with the 6-311++G(2d,2p) basis. This value should be compared with the experimental one, which lies between 3.1 and 3.57[48] D, and with the CCSD-(T)/ 6-311++G(2d,2p) computed value of 3.59 D.[44]

The bond dissociation energies are provided in Table 4. To include the zero-point energy (ZPE) correction, we have optimized the open-shell fragments CH_3 and NO_2. For MCSCF the point at R(C−N) = 4.00 Å was taken as the dissociation limit. As shown in the table, the density functional results are very comparable to that of QCISD and MCSCF. With the larger basis, the dissociation energy improved on the order of 0.6−3.0 kcal/mol, depending on the computational method used. The DFT(B3PW91) and MCSCF results of this basis are approximately 5 kcal/mol lower than the experimental values of 59−60 kcal/mol.[49,50] This deviation is not unexpected from calculations of the type reported in this work. The MRD-CI calculations of Roszak and Kaufman,[28] which also included a generalized multireference Davidson correction formula, gave a value of 64.3 kcal/mol. The limited sizes of the basis sets employed might be one source for the discrepancy between the computational and experimental results, and inclusion of f-type and higher order basis functions could lead to a better agreement.

On the other hand, we note that the experimentally determined zero-point energy correction (ZPE) for CH_3NO_2, CH_3, and NO_2 are 30.3, 16.2, and 5.4 kcal/mol, respectively.[51,52] Our calculated values in this work at the 6-311G** QCISD level are 31.8 (CH_3-NO_2), 18.7 (CH_3), and 5.8 (NO_2) and at the 6-311++G(2d,2p) DFT(B3PW91) level are 31.3 (CH_3NO_2), 18.6 (CH_3), and 5.6 kcal/mol for NO_2. Thus, approximately up to 2.5 kcal/mol difference could be attributed to error in determining the ZPE correction of CH_3. This could be due in part to the explicit assumption of the validity of the harmonic approximation. Contributions from cubic and quartic anharmonic terms for this molecule are very significant, as was shown by Schatz et al.[53] Furthermore, one-point calculations using the experimental geometrical parameters and ZPEs for NO_2 and CH_3 species while fixing R(C−N) at 8.00 Å improved the dissociation energy to 56.2 kcal/mol at the 6-311++G(2d,2p) MCSCF level of theory.

Figure 2 illustrates the calculated potential energy curves from MCSCF and QCISD methods. Figure 3 shows the relative energies obtained from DFT calculations to those of MCSCF. While the energy difference seems to be systematic for all functionals, the potential energy curves predicted by the BLYP and BPW91 methods are strikingly broader than those predicted by the high-level methods. At R(C−N) = 2.25 Å, the BLYP energy is about 17 kcal/mol lower than the MCSCF value and 13 kcal/mol lower than the corresponding QCISD value. It is

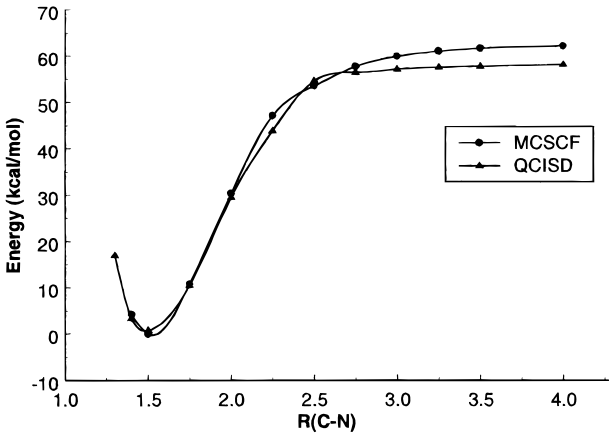

Figure 2. Fully optimized MCSCF and QCISD ground-state potential energy curves for nitromethane.

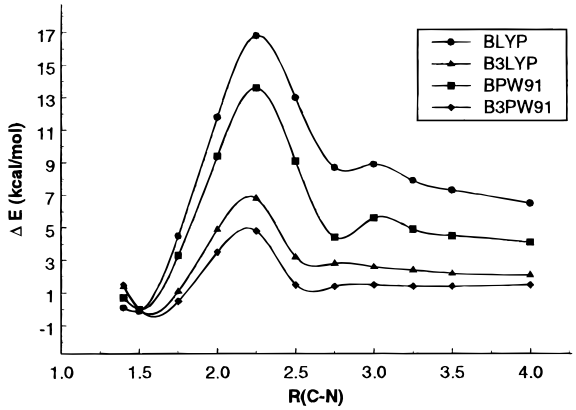

Figure 3. Calculated energy difference ΔE [E(MCSCF) − E(DFT)] of the singlet potential curve.

also noticed that this effect persists, albeit with relatively lower deviation, throughout the dissociation pathway up to R(C−N) = 3.0 Å. With this anharmonic deviation, the calculated force constant will be weakened considerably and effects on calculated properties such as frequency shifts would be notable. The B3PW91 and B3LYP functionals predict dissociation curves in better agreement with those of MCSCF and QCISD calculations. As can be seen from Figure 3, the maximum energy deviation of B3PW91 and B3LYP from MCSCF is 4 and 7 kcal/mol at R(C−N) = 2.25 Å, respectively.

In Table 5 the geometrical parameters from representative calculations are provided. In the illustrated region, we note that the bond lengths R(C−H) and R(N−O) follow the order MCSCF < B3PW91 ∼ B3LYP < QCISD < BPW91 ∼ BLYP, while the bond angles ONO, HCH, and CNO show little change as a function of the method used. In all, the geometrical structure throughout the dissociation process tends to remain in the C_s symmetry. The CH_3 moiety changes from the pyramidal structure in the bonded molecule to planar as a free fragment. The geometric parameters of the fragment species are correctly reproduced at the end of the decomposition and should be compared with the literature values R(N−O) = 1.194 Å, ∠ONO = 133.8° for NO_2,[54] and R(C−H) = 1.079 Å for CH_3.[55] Both the ∠ONO and ∠HCH angles vary by roughly 10° in going from the equilibrium structure of nitromethane to the end of the dissociation. We note that the use of the larger basis has little effect on the molecular geometrical parameters as determined at the MCSCF and DFT(B3LYP) levels of theory. Finally, as expected, both DFT and QCISD wave functions exhibit significant spin contamination due to mixing with the

TABLE 5: Geometries and Energy Differences[a] for the Singlet State Predicted with the 6-311G Basis by MCSCF, QCISD, and B3PW91 Methods (Top to Bottom, Respectively)**

	R(C−N)						
	1.40	1.50	1.75	2.00	2.25	2.50	2.75
$R(C-H_1)$	1.081	1.077	1.075	1.074	1.074	1.085	1.083
	1.093	1.092	1.088	1.086	1.085	1.085	1.083
	1.088	1.087	1.086	1.084	1.083	1.082	1.082
$R(C-H_{2,3})$	1.078	1.078	1.076	1.075	1.074	1.074	1.074
	1.089	1.088	1.087	1.086	1.085	1.085	1.083
	1.087	1.086	1.085	1.083	1.082	1.082	1.081
$R(N-O)$	1.202	1.198	1.191	1.185	1.176	1.169	1.167
	1.220	1.219	1.209	1.206	1.202	1.207	1.195
	1.221	1.219	1.209	1.206	1.202	1.207	1.195
	1.221	1.215	1.204	1.197	1.195	1.194	1.193
$\angle H_2CH_1$	109.4	110.8	113.7	115.8	117.0	117.7	118.5
	109.2	110.8	113.3	115.8	117.6	119.1	119.8
	111.8	112.9	114.9	116.8	118.2	119.3	119.8
$\angle NCH_1$	108.5	107.2	104.1	101.6	99.8	98.7	97.4
	107.7	106.6	104.5	100.8	97.7	93.7	92.6
	109.5	107.9	103.8	101.0	98.5	95.7	93.5
$\angle CNO_1$	117.8	117.2	116.3	115.6	114.5	115.0	114.4
	117.5	116.9	116.5	116.1	115.1	115.1	113.0
	117.6	117.1	116.4	115.5	115.0	114.2	113.7
$\angle ONO$	124.4	125.5	127.3	128.9	131.0	133.2	134.1
	125.3	126.1	128.1	128.5	130.1	129.6	133.8
	125.0	126.1	128.2	129.6	130.4	131.5	132.4
$\angle\phi$	2.4	2.1	1.4	0.8	0.5	0.3	0.1
	2.6	2.4	0.1	0.2	0.2	0.0	0.0
	2.3	2.0	0.1	0.2	0.1	0.1	0.1
ΔE_e	4.3	0.0	10.8	30.3	47.1	53.5	57.7
	3.4	0.8	10.5	29.5	43.8	54.6	56.4
	2.8	0.0	10.3	26.8	42.3	52.0	56.3

[a] Bond lengths in Å and angles in degrees. Energies are in kcal/mol relative to the respective equilibrium structure.

triplet surface, starting at $R(C-N) = 2.75$ Å where the S^2 value is 0.975 and 0.751 from B3PW91 and QCISD, respectively. At $R(C-N) = 4.00$ Å the spin contamination is most pronounced with S^2 being from the two methods 1.03 and 1.0, respectively.

Conclusion

In this paper we have undertaken a comparative study of C−N bond dissociation for the singlet and triplet states of nitromethane, a prototypical energetic material. In addition to characterizing the triplet state minimum energy structure, we have found that the potential energy curve for this state exhibits an energy barrier that is 33 kcal/mol as determined at the MCSCF level. This barrier renders the state bound with respect to decomposition into CH_3 and NO_2 fragments, and its relevance in photodissociation studies should be considered. The DFT results locate the barrier around $R(C-N) = 1.75$ Å, shorter than the MCSCF value at $R(C-N) = 2.0$ Å. DFT methods also predict a lower energy barrier with the B3LYP functional showing closer agreement with MCSCF than the BLYP.

The equilibrium properties of the singlet state predicted by all methods, including bond lengths, angles, and dipole moment, were in close agreement with experiment and a CCSD(T)[44] calculation. Good agreement for the potential energy along the reaction coordinate was found between the MCSCF and the QCISD methods for bond distances less than 2.75 Å. The difference between the DFT and MCSCF results was found to have a distinct maximum near $R(C-N) = 2.25$ Å for all methods studied. DFT methods should be used with caution in this region, which corresponds to the onset of bond cleavage. The difference, however, decreased at larger bond distances.

Overall, we find that the DFT methods based on Becke's 3-parameter exchange functional faired best in the comparison to high-level methods. The correlation functional played a less dominant role. The difference in energy between 6 and 311G** and 6-311++G(2d,2p) was less than 1 kcal/mol for the B3LYP and B3PW91 functionals. We conclude that either the B3PW91/6-311G** or B3LYP/6-311G** DFT method should be accurate to within 5 kcal/mol for the treatment of homolytic bond cleavage of closed-shell energetic materials similar to nitromethane. These methods also reproduce the qualitative features of open-shell systems but showed errors of up to 12 kcal/mol in predicted barrier heights. This level of accuracy is sufficient to distinguish between competing reaction channels with widely ranging energetics.[2]

Acknowledgment. This work was performed under the auspices of the U.S. Department of Energy by the Lawrence Livermore National Laboratory under Contract No. W-7405-Eng-48.

References and Notes

(1) Rice, B. M.; Chabalowski, C. F. *J. Phys. Chem. A* **1997**, *101*, 8720.
(2) Wu, C. J.; Fried, L. E. *J. Phys. Chem.* **1997**, *101*, 8675.
(3) Curtiss, L. A.; Raghavachari, K.; Redfern, P. C.; Pople, J. A. *J. Chem. Phys.* **1996**, *106*, 1063.
(4) Kohn, W.; Becke, A. D.; Parr, R. G. *J. Phys. Chem.* **1996**, *100*, 12974.
(5) Johnson, B. G.; Gonzales, C. A.; Gill, P. M. W.; Pople, J. A. *Chem. Phys. Lett.* **1994**, *221*, 100.
(6) Johnson, B. G.; Gill, P. M. W.; Pople, J. A. *J. Chem. Phys.* **1993**, *98*, 5612.
(7) Handy, N. C.; Murray, C. W.; Amos, R. D. *J. Phys. Chem.* **1993**, *97*, 4392.
(8) Estrin, D. A.; Paglieri, L.; Corongiu, G. *J. Phys. Chem.* **1994**, *98*, 5653.
(9) Carpenter, J. E.; Sosa, C. P. *J. Mol. Struct.* **1994**, *311*, 325.
(10) Pai, S. V.; Chabalowski, C. F.; Rice, B. M. *J. Phys. Chem.* **1996**, *100*, 15368, **1997**, 101, 3400 and references therein.
(11) Cramer, C. J.; Dulles, F. J.; Storer, J. W.; Worthington, S. E. *Chem. Phys. Lett.* **1994**, *218*, 387.
(12) Mebel, A. M.; Luna, A.; Lin, M. C.; Morokuma, K. *J. Chem. Phys.* **1996**, *105*, 6439.
(13) Sicilia, E.; Toscano, M.; Mineva, T.; Russo, N. *Int. J. Quantum Chem.* **1997**, *61*, 571.
(14) Queralt, J. J.; Safont, V. S.; Moliner, V.; Andres, J. *Theor. Chim. Acta* **1996**, *94*, 247.
(15) Irigoras, A.; Ugalde, J. M.; Lopez, X.; Sarasola, C. *Can. J. Chem.* **1996**, *74*, 1824.
(16) Blais, N. C.; Engelke, R.; Sheffield, S. A. *J. Phys. Chem*. A **1997**, *101*, 8285.
(17) Winey, J. M.; Gupta, Y. M. *J. Phys. Chem*. B **1997**, *101*, 10733.
(18) Gruzdkov, Y. A.; Gupta, Y. M. *J. Phys. Chem*. A **1998**, *102*, 2322.
(19) Hill, J. R.; Moore, D. S.; Schmidt, S. C.; Storm, C. B. *J. Phys. Chem.* **1991**, *95*, 3039.
(20) Miller, P. J.; Block, S.; Piermarini, G. J. *J. Phys. Chem.* **1989**, *93*, 462.
(21) Renlund, A. M.; Trott, W. M. In *Shock Compression of Condensed Matter;* Schmidt, S. C., Johnson, J. N., Davison, J. W., Eds.; Elsevier: New York, 1990.
(22) Pangilinan, G. I.; Gupta, Y. M. *J. Phys. Chem.* **1994**, *98*, 4522.
(23) Moss, D. B.; Trentelman, K. A.; Houston, P. L. *J. Chem. Phys.* **1992**, *96*, 237, and references therein.
(24) Flicker, W. M.; Mosher, O. A.; Kuppermann, A. *Chem. Phys. Lett.* **1979**, *60*, 518.
(25) Honda, K.; Mikuni, H.; Takahasi, M. *Bull. Chem. Soc. Jpn.*. **1972**, *45*, 3534.
(26) Rajchenbach, C.; Jonusauskas, G.; Rulliere, C. *Chem. Phys. Lett*. **1995**, *231*, 467.
(27) Jursic, B. S. *Int. J. Quantum Chem*. **1997**, *64*, 263.
(28) Roszak, S.; Kaufman, J. J. *J. Chem. Phys.* **1991**, *94*, 6030.
(29) Seminario, J. M.; Concha, M. C.; Politzer, P. *J. Chem. Phys.* **1995**, 102, 8281. (b) Seminario, J. M.; Concha, M. C.; Politzer, P. *Int. J. Quantum Chem. Symp. 29* **1995**, 621.
(30) Tuckerman, M. E.; Klein, M. L. *Chem. Phys. Lett*. **1998**, *283*, 147.
(31) Rice, B. M.; Thompson, D. L. *J. Chem. Phys*. **1990**, *93*, 7986 (and references therein).
(32) Politzer, P.; Seminario, J. M.; Zacarias, A. G. *Mol. Phys*. **1996**, *89*, 1511.
(33) Saxon, R. P.; Yoshimine, M. *Can. J. Chem*. **1992**, *70*, 572.

(34) Roos, B. O. In *Advances in Chemical Physics*, Lawley, K. P., Ed.; Wiley-Interscience: New York, 1987; p 69.

(35) Pople, J. A.; Head-Gordon, M.; Raghavachari, K. J. *J. Chem. Phys.* **1987**, *87*, 5968.

(36) Manaa, M. R.; Fried, L. E. Manuscript in preperation.

(37) Frisch, M. J.; Trucks, G. W.; Schlegel, H. B.; Gill, P. M. W.; Johnson, B. G.; Robb, M. A.; Cheeseman, J. R.; Kieth, T.; Petersson, G. A.; Montgomery, J. A.; Raghavachari, K.; Al-Laham, M. A.; Zakrzewski, V. G.; Ortiz, J. V.; Foresman, J. B.; Cioslowski, J.; Stefanov, B. B.; Nanayakkara, A.; Challacombe, M.; Peng, C. Y.; Ayala, P. Y.; Chen, W.; Wong, M. W.; Andres, J. L.; Replogle, E. S.; Gomperts, R.; Martin, R. L.; Fox, D. J.; Binkley, J. S.; Defrees, D. J.; Baker, J.; Stewart, J. P.; Head-Gordon, M.; Gonzales, C.; Pople, J. A. *Gaussian 94*, revision E.2; Gaussian, Inc.: Pittsburgh, PA, 1995.

(38) Becke, A. D. *J. Chem. Phys.* **1993**, *98*, 5648.

(39) Perdew, J. P.; Wang, Y. *Phys. Rev. B* **1992**, *45*, 13244.

(40) Lee, C.; Yang, W.; Parr, R. G. *Phys. Rev. B* **1988**, *37*, 785.

(41) Becke, A. D. *Phys. Rev. A* **1988**, *38*, 3098.

(42) Schmidt, M. W.; Baldridge, K. K.; Boatz, J. A.; Elbert, S. T.; Gordon, M. S.; Jensen, J. H.; Koseki, S.; Matsunaga, N.; Nguyen, K. A.; Su, S. J.; Windus, T. L.; Dupuis, M.; Montgomery, J. A. *J. Comput. Chem.* **1993**, *14*, 1347.

(43) Marynick, D. S.; Ray, A. K.; Fry, J. L.; Kleier, D. A. *J. Mol. Struct. (THEOCHEM)* **1984**, *108*, 45.

(44) Gutsev, G. L.; Bartlett, R. J. *J. Chem. Phys.* **1996**, *105*, 8785.

(45) Gilbert, B. C.; Trenwith, M. *J. Chem. Soc., Perkins Trans. 2* **1973**, 2010.

(46) Romondo, F. *Can. J. Chem.* **1992**, *70*, 314.

(47) Lobo, R. F. M.; Moutinho, A. M. C.; Lacmann, K.; Los, J. *J. Chem. Phys.* **1991**, *95*, 166.

(48) McClellan, A. L. *Tables of Experimental Dipole Moments*, Freeman: San Fransisco, CA, 1963.

(49) Benson, S. W.; O'Neal, H. E. *Kinetic Data on Gas-Phase Unimolecular Reactions*; National Standard Reference Data Series, National Bureau of Standards: Washington, DC, 1970.

(50) Pedley, J. B.; Naylor, R. D.; Kirby, S. P. *Thermochemical Data of Organic Compounds*, 2nd ed.; Chapman: New York, 1986.

(51) Gorse, D.; Cavagnat, D.; Pesquer, M.; Lapouge, C. *J. Phys. Chem.* **1993**, *97*, 4262.

(52) Chase, M. W., Jr.; Davies, C. A.; Downey, J. R., Jr.; Frurip, D. J.; McDonald, R. A.; Syverud, A. N. *JANAF Thermochemical Tables*, 3rd ed. *J. Phys. Chem. Ref. Data, Suppl.* **1985**, *14* (1).

(53) Schatz, G. C.; Wagner, A. F.; Dunning, T. H. *J. Phys. Chem*. **1984**, *88*, 221.

(54) Kaldor, U. *Chem. Phys. Lett*. **1991**, *185*, 131.

(55) Spirko, V.; Bunker, P. R. *J. Mol. Spectrosc*. **1982**, *95*, 381.